Monthly Notices
of the
ROYAL ASTRONOMICAL SOCIETY

Mon. Not. R. Astron. Soc. **405,** 2345–2350 (2010) doi:10.1111/j.1365-2966.2010.16665.x

A computed line list for the H_2D^+ molecular ion

Taha Sochi★ and Jonathan Tennyson★

Department of Physics and Astronomy, University College London, Gower Street, London WC1E 6BT

Accepted 2010 March 9. Received 2010 March 9; in original form 2010 February 9

ABSTRACT

A comprehensive, calculated line list of frequencies and transition probabilities for the singly deuterated isotopologue of H_3^+, H_2D^+, is presented. The line list, called ST1, contains over 22 million rotational-vibrational transitions occurring between more than 33 thousand energy levels; it covers frequencies up to 18 500 cm^{-1}. All energy levels with rotational quantum number, J, up to 20 are considered, making the line list useful for temperatures up to at least 3000 K. About 15 per cent of these levels are fully assigned with approximate rotational and vibrational quantum numbers. The list is calculated using a previously proposed, high accuracy, *ab initio* model and consistency checks are carried out to test and validate the results. These checks confirm the accuracy of the list. A temperature-dependent partition function, valid over a more extended temperature range than those previously published, and cooling function are presented. Temperature-dependent synthetic spectra in the frequency range 0–10 000 cm^{-1} are also given.

Key words: atomic processes – molecular data – methods: numerical – techniques: spectroscopic – early Universe – infrared: ISM.

1 INTRODUCTION

H_2D^+ is one of the simplest polyatomic quantum systems. It consists of two electrons bound to three nuclei (two protons and one deuteron) forming a triangular shape at equilibrium. The molecule is an asymmetric prolate top with three vibrational modes: breathing (ν_1), bending (ν_2) and asymmetric stretch (ν_3). All these modes are infrared active. H_2D^+ also possesses a permanent electric dipole moment of about 0.6 D due to the displacement of the centre of charge from the centre of mass. Hence pure rotational transitions, which occur in the far-infrared, can occur. This all contrasts strongly with the non-deuterated H_3^+ molecular ion which has no allowed rotational spectrum and only one infrared active vibrational mode.

In astrophysical environments, H_2D^+ is formed by several reactions; the main one is

$$H_3^+ + HD \rightarrow H_2D^+ + H_2. \quad (1)$$

As this and other similar formation reactions are exothermic, the formation of H_2D^+ in the cold interstellar environment is favoured. Consequently, the abundance of this species can be greatly enhanced compared to the underlying D/H ratio. As an isotopologue of H_3^+, H_2D^+ is a major participant in chemical reactions taking place in interstellar medium (ISM). In particular, it plays a key role in the deuteration processes in these environments (Millar 2003). Because H_3^+ lacks a permanent dipole moment and hence cannot be detected via radio astronomy, its asymmetrical isotopomers, namely H_2D^+ and D_2H^+, are the most promising tracers of the extremely cold and highly dense interstellar clouds. These species are the last to remain in gaseous state under these extreme conditions with observable pure rotational spectra (Dalgarno et al. 1973; Herbst & Millar 2008). Of these two isotopomers, H_2D^+ is the more abundant and easier to observe and hence it is the main species to utilize in such astrophysical investigations.

Although the existence of H_2D^+ in the ISM and astrophysical objects was contemplated decades ago (Dalgarno et al. 1973; van Dishoeck et al. 1992) with some reported tentative sighting (Phillips et al. 1985; Pagani et al. 1992; Boreiko & Betz 1993), it is only relatively recently that the molecule was firmly detected in the ISM via one of its rotational transition lines (Stark, van der Tak & van Dishoeck 1999). There have been many subsequent astronomical studies of H_2D^+ spectra (Caselli et al. 2003; Ceccarelli et al. 2004; Stark et al. 2004; Vastel, Phillips & Yoshida 2004; Harju et al. 2006; Hogerheijde et al. 2006; Cernicharo, Polehampton & Goicoechea 2007; Caselli et al. 2008). In particular these spectra have been used to investigate the mid-plane of protoplanetary discs (Ramos, Ceccarelli & Elitzur 2007), the kinematics of the centres of pre-stellar cores (van der Tak, Caselli & Ceccarelli 2005), and the suggestion of possible use as a probe for the presence of the hypothetical cloudlets forming the baryonic dark matter (Ceccarelli & Dominik 2006). Vibrational transitions of H_2D^+ have yet to be observed astronomically.

The potential importance of H_2D^+ spectroscopy for cosmology is obvious as it is a primordial molecular species which could have a considerable abundance in the early Universe. In particular it has a potential role in the cooling of primordial proto-objects

★E-mail: t.sochi@ucl.ac.uk (TS); j.tennyson@ucl.ac.uk (JT)

(Dubrovich 1993; Dubrovich & Lipovka 1995; Galli & Palla 1998; Dubrovich & Partridge 2000; Schleicher et al. 2008). Its significance is highlighted by a number of studies which consider the role of H_2D^+ in spectral distortions of cosmic microwave background radiation and whether this can be used to determine the H_2D^+ and deuterium abundances at different epochs (Dubrovich & Lipovka 1995). Finally the H_2D^+ 372 GHz line has been considered as a probe for the presence of dark matter (Ceccarelli & Dominik 2006).

Due to its fundamental and astrophysical importance, H_2D^+ has been the subject of a substantial number of spectroscopic studies. The first successful spectroscopic investigation of H_2D^+ was carried out by Shy, Farley & Wing (1981) where nine rotational-vibrational transitions were measured in the infrared region between 1800 and 2000 cm^{-1} using Doppler-tuned fast-ion laser technique, but no specific spectroscopic assignments were made. This was followed by other spectroscopic investigations which include the observation and identification of the strong and highly important rotational 1_{10}–1_{11} transition line of ortho-H_2D^+ at 372 GHz by Bogey et al. (1984) and Warner et al. (1984). Amano & Hirao (2005) measured the frequency of the 1_{10}–1_{11} line of H_2D^+ with improved accuracy, as well as the 3_{21}–3_{22} line at 646.430 GHz. The three fundamental vibrational bands of the H_2D^+ ion were observed by Amano & Watson (1984), Amano (1985) and Foster et al. (1986) using laser spectroscopy. Fárník et al. (2002) measured transitions to overtones $2\nu_2$ and $2\nu_3$ and to combination $\nu_2 + \nu_3$ in jet-cooled H_2D^+ ions. Hlavenka et al. (2006) measured second overtone transition frequencies of H_2D^+ using cavity ringdown absorption spectroscopy. Other spectroscopic investigations include those of Asvany et al. (2007), who detected 20 lines using laser induced reaction techniques, and the recent work of Yonezu et al. (2009), who reported precise measurement of the transition frequency of the H_2D^+ 2_{12}–1_{11} line at 2.363 THz, alongside three more far-infrared lines of H_2D^+, using tunable far-infrared spectrometry. However, none of these studies measured absolute line intensities, although the work of Fárník et al. (2002) and Asvany et al. (2007) give relative intensities.

Several synthetic, H_2D^+ line lists have been generated from *ab initio* calculations. Prominent examples include the line list of Miller, Tennyson & Sutcliffe (1989) and another one generated as part of the work reported by Asvany et al. (2007). Miller et al. list extends to rotational level $J = 30$ and covers all levels up to 5500 cm^{-1} above the ground state. These lists were used in a number of studies for various purposes such as spectroscopic assignment of energy levels and transition lines from astronomical observations, and for computation of a low-temperature partition function (Sidhu, Miller & Tennyson 1992). The line lists also played an important role in motivating and steering the experimental and observational work in this field (Miller et al. 1989; Asvany et al. 2007). None the less, the previous H_2D^+ line lists suffered from limitations that include low-energy cut-off and the inclusion of a limited number of levels especially at high J. These limitations, alongside the development of high-accuracy *ab initio* models of H_3^+ and its isotopologues, including H_2D^+, by Polyansky & Tennyson (1999), provided the motivation to generate a more comprehensive and accurate line list. The intention is that the new list will both fill the previous gaps and provide data of better quality.

The line list, which we call ST1, consists of 22 164 810 transition lines occurring between 33 330 rotational-vibrational levels. These are all the energy levels with rotational quantum number $J \leq 20$ and frequencies below 18 500 cm^{-1}. This line list can be seen as a companion to the H_3^+ line list of Neale, Miller & Tennyson (1996) which has been extensively used for astrophysical studies; although for reasons explained below, the ST1 line list is actually expected to be more accurate.

2 METHOD

Vibration–rotation calculations were performed using the DVR3D code of Tennyson et al. (2004). The code calculates, among other things, wavefunctions, energy levels, transition lines, dipole moments and transition probabilities. DVR3D uses an exact Hamiltonian, within the Born–Oppenheimer approximation, and requires potential energy and dipole surfaces to be supplied as input. In general, it is these which largely determine the accuracy of the resulting calculations (Polyansky et al. 2003).

The vibrational stage of the DVR3D suite requires an accurate model for the variation of electronic potential as a function of nuclear geometry. Here we use the H_3^+ global potential surface of Polyansky et al. (2000), which used the ultrahigh accurate *ab initio* data of Cencek et al. (1998) supplemented by extra data points; the surface was constrained at high energy by the data of Schinke, Dupuis & Lester (1980). We added the H_2D^+ adiabatic correction term fitted by Polyansky & Tennyson (1999) to this surface. We also employed Polyansky & Tennyson's vibrational mass scaling to allow for non-adiabatic corrections to the Born–Oppenheimer approximation: we used $\mu_H = 1.007\,5372$ u and $\mu_D = 2.013\,8140$ u for the vibrational atomic masses, and $\mu_H = 1.007\,276\,47$ u and $\mu_D = 2.013\,553\,20$ u for the rotational atomic masses. The accuracy of this model is assessed below.

Calculations were performed in Jacobi coordinates (r_1, r_2, θ), where r_1 represents the diatom distance (H–H), r_2 is the separation of the D atom from the centre of mass of the diatom, and θ is the angle between r_1 and r_2. Radial basis functions of Morse oscillator type were used to model r_1 (Tennyson & Sutcliffe 1982), while spherical oscillators were used to model r_2 (Tennyson & Sutcliffe 1983). Following Polyansky & Tennyson (1999), the Morse parameters for r_1 were set to $r_e = 1.71$, $D_e = 0.10$ and $\omega_e = 0.0108$, with 20 Gauss–Laguerre grid points. Parameters of the spherical oscillator functions were set to $\alpha = 0.0$ and $\omega_e = 0.0075$ with 44 Gauss–Laguerre grid points, following extensive tests on convergence of the vibrational band origins. 36 Gauss–Legendre grid points were used to represent the angular motion. The final vibrational Hamiltonian matrix used was of dimension 2000.

In the rotation stage, the size of the Hamiltonian matrix, which is a function of J, was set to $1800(J + 1)$ following tests on $J = 3$ and 15. These tests demonstrated that choosing sufficiently large values for the rotational Hamiltonian, although computationally expensive, is crucial for obtaining reliable results. Our aim was to obtain convergence to within 0.01 cm^{-1} for all rotation-vibration levels considered. Our tests suggest we achieved this except, possibly, for some of the highest lying levels. For these levels our basic model, and in particular our corrections to the Born–Oppenheimer approximation, are not reliable to this accuracy.

To compute the intensity of the vibration–rotation transitions, a dipole moment surface is required. We used the *ab initio* dipole surface of Röhse et al. (1994) to calculate the components of the H_2D^+ dipole. In the DIPOLE3 module of DVR3D we set the number of Gauss–Legendre quadrature points used for evaluating the wavefunctions and dipole surface to 50; this choice is consistent with the requirement that this parameter should be slightly larger than the number of DVR points used to calculate the underlying wavefunctions.

The final ST1 line list consists of two main files: one for the levels and the other for the transitions. These two files are constructed and

Table 1. Sample of the ST1 levels file. The columns from left- to right-hand side are for index of level in file, J, symmetry, index of level in block, frequency in cm^{-1}, v_1, v_2, v_3, J, K_a and K_c. We used -2 to mark unassigned quantum numbers.

730	1	4	99	18 265.615 25	−2	−2	−2	1	1	0
731	1	4	100	18 379.999 89	−2	−2	−2	1	1	0
732	1	4	101	18 499.057 36	−2	−2	−2	1	1	0
733	2	1	1	131.634 73	0	0	0	2	0	2
734	2	1	2	223.863 06	0	0	0	2	2	0
735	2	1	3	2318.350 91	0	1	0	2	0	2
736	2	1	4	2427.092 31	0	1	0	2	2	0
737	2	1	5	2490.933 74	0	0	1	2	1	2
738	2	1	6	3123.279 57	1	0	0	2	0	2
739	2	1	7	3209.806 78	1	0	0	2	2	0

Table 2. Sample of the ST1 transitions file. The first two columns are for the indices of the two levels in the levels file, while the third column is for the A coefficients in s^{-1}.

30 589	29 553	7.99E−04
19 648	18 049	8.37E−03
8943	7423	5.55E−01
8490	7981	2.18E−03
20 620	22 169	6.91E−04
17 613	15 937	5.62E−03
13 046	11 400	1.15E−00
20 639	20 054	7.26E−03
14 433	17 117	2.49E−03
25 960	28 074	1.92E−03

formatted according to the method and style of the BT2 water line list (Barber et al. 2006). The total amount of CPU time spent in producing the ST1 list including preparation, convergence tests and verifying the final results is about 8000 hours. We used the serial version of the DVR3D suite on PC platforms running Linux (Red Hat) operating system. Both 32- and 64-bit machines were used in this work although the final data were produced mainly on 64-bit machines due to the large memory requirement for the high-J calculations.

This variational nuclear motion procedure used for the calculations provides rigorous quantum numbers: J, ortho/para and parity p, but not the standard approximate quantum numbers in normal mode, rigid rotor notation. We hand labelled those levels for which such quantum numbers could be assigned in a fairly straightforward fashion. 5000 of these levels are fully designated with three rotational (J, K_a, K_c) and three vibrational (v_1, v_2, v_3) quantum numbers, while 341 levels are identified with rotational quantum numbers only. Some of these assignments are made as initial guess and hence should be treated with caution. Tables 1 and 2 present samples of the ST1 levels and transitions files, respectively.

3 RESULTS AND VALIDATION

3.1 Comparison to Experimental and Theoretical Data

We made a number of comparisons between the ST1 line list and laboratory data found in the literature. This enabled us to validate our results. The main sources of laboratory measurements that we used in our comparisons are presented in Table 3. The table also gives statistical information about the discrepancy between our calculated line frequencies and their experimental counterparts. Table 4 presents a rather detailed account of this comparison for a sample data extracted from one of these data sets, specifically that of Asvany et al. (2007). This table also contains a comparison of relative Einstein B coefficients between theoretical values from ST1 and measured values from Asvany et al. The theoretical values in this table are obtained from the calculated A coefficients using the relation

$$B_{lu} = \frac{(2J' + 1)c^3 A_{ul}}{(2J'' + 1)_l 8\pi h \nu^3}, \tag{2}$$

where A_{ul} and B_{lu} are the Einstein A and B coefficients, respectively, for transition between upper (u) and lower (l) states, J' and J'' are the rotational quantum numbers for upper and lower states, h is Planck's constant and ν is the transition frequency.

As seen, the ST1 values agree with the measured coefficients of Asvany et al. to within experimental error in all cases. Other comparisons to previous theoretical data, such as that of Polyansky & Tennyson (1999), were also made and the outcome was satisfactory in all cases.

3.2 Partition function

The partition function of a system consisting of an ensemble of particles in thermodynamic equilibrium is given by

$$z(T) = \sum_i (2J_i + 1) g_i e^{-E_i/(kT)}, \tag{3}$$

where i is an index running over all energy states of the ensemble, E_i is the energy of state i above the ground level which has rotational angular momentum J_i, k is Boltzmann's constant, T is temperature, and g_i is the nuclear spin degeneracy factor which is 1 for para states and 3 for ortho ones.

Using the ST1 energy levels we calculated the partition functions of H_2D^+ for a range of temperatures and compared the results to those obtained by Sidhu et al. (1992). Table 5 presents these results for a temperature range of 5–4000 K. The results are also graphically presented in Fig. 1. The table and figure reveal that although our results and those of Sidhu et al. agree very well at temperatures below 1200 K, they differ significantly at high temperatures and the deviation increases as the temperature rises. This can be explained by the fact that ST1 contains more energy levels which contribute increasingly at high temperatures. We therefore expect our partition function to be the more reliable one for $T > 1200$K.

Using a Levenberg–Marquardt non-linear curve-fitting routine, we fitted the ST1 partition function curve to a fifth-order polynomial

$$z(T) = \sum_{i=0}^{5} a_i T^i \tag{4}$$

in temperature and obtained the following coefficients for T in K:

$$\begin{aligned} a_0 &= -0.300\,315, \\ a_1 &= +0.094\,722, \\ a_2 &= +0.000\,571, \\ a_3 &= -3.244\,15 \times 10^{-7}, \\ a_4 &= +2.012\,40 \times 10^{-10}, \\ a_5 &= -1.941\,76 \times 10^{-14}. \end{aligned} \tag{5}$$

This polynomial is not shown in Fig. 1 because it is virtually identical to the ST1 curve.

Table 3. Main experimental data sources used to validate the ST1 list. Columns 2 and 3 give the number of data points and the frequency range of the experimental data, respectively, while the last three columns represent the minimum, maximum and standard deviation of discrepancies (i.e. observed minus calculated) in cm^{-1} between the ST1 and the experimental data sets.

Source	N	Range (cm^{-1})	Minimum	Maximum	σ
Shy et al. (1981)	9	1837–1953	−0.014	0.116	0.052
Amano & Watson (1984)	27	2839–3179	−0.315	0.054	0.065
Amano (1985)	37	2839–3209	−0.024	0.054	0.019
Foster et al. (1986)	73	1837–2603	−0.134	0.213	0.067
Fárník et al. (2002)	8	4271–4539	0.046	0.172	0.050
Asvany et al. (2007)	25	2946–7106	0.008	0.242	0.088

Table 4. Comparison between measured (Asvany et al. 2007) and calculated (ST1) frequencies and relative Einstein B coefficients for a number of transition lines of H_2D^+. These coefficients are normalized to the last line in the table. The absolute B coefficients, as obtained from the A coefficients of ST1 list using equation (2), are also shown in column 5 as multiples of 10^{14} and in units of $str.s.kg^{-1}$.

Transition		Freq. (cm^{-1})		B	Relative B	
Vib.	Rot.	Obs.	ST1	ST1	Obs.	ST1
(0,3,0)	$1_{10} \leftarrow 1_{11}$	6303.784	6303.676	8.05	0.29	0.29
(0,3,0)	$1_{01} \leftarrow 0_{00}$	6330.973	6330.850	8.59	0.32±0.02	0.31
(0,2,1)	$0_{00} \leftarrow 1_{11}$	6340.688	6340.456	7.36	0.27±0.03	0.27
(0,2,1)	$2_{02} \leftarrow 1_{11}$	6459.036	6458.794	9.17	0.35±0.04	0.34
(0,2,1)	$1_{11} \leftarrow 0_{00}$	6466.532	6466.300	27.3	1.00	1.00

Table 5. Partition functions of H_2D^+ for a number of temperatures as obtained from Sidhu et al. (1992) and ST1 line lists.

T (K)	Partition function		T (K)	Partition function	
	Sidhu	ST1		Sidhu	ST1
5	1.00	1.00	800	347.58	347.53
10	1.01	1.01	900	426.24	426.24
20	1.07	1.28	1000	515.43	516.31
30	2.15	2.15	1200	731.43	737.61
40	3.46	3.46	1400	1004.25	1026.84
50	5.05	5.05	1600	1339.43	1401.52
60	6.82	6.82	1800	1738.89	1881.33
70	8.73	8.73	2000	2203.94	2487.98
80	10.76	10.76	2200	2735.31	3244.83
90	12.90	12.89	2400	3327.58	4176.19
100	15.12	15.12	2600	3983.83	5306.36
150	27.56	27.55	2800	4698.51	6658.69
200	42.03	42.02	3000		8254.62
300	76.49	76.46	3200		10 112.90
400	117.48	117.44	3400		12 249.00
500	164.51	164.53	3600		14 674.90
600	218.11	217.98	3800		17 398.90
700	278.66	278.58	4000		20 425.60

3.3 Cooling function

ST1 was also used to compute the cooling function of H_2D^+ as a function of temperature. The cooling function W which quantifies the rate of cooling per molecule for dense gas in local thermodynamic equilibrium is given by

$$W(T) = \frac{1}{z}\left[\sum_{u,l} A_{ul}(E_u - E_l)(2J_u + 1)g_u e^{-E_u/(kT)}\right], \quad (6)$$

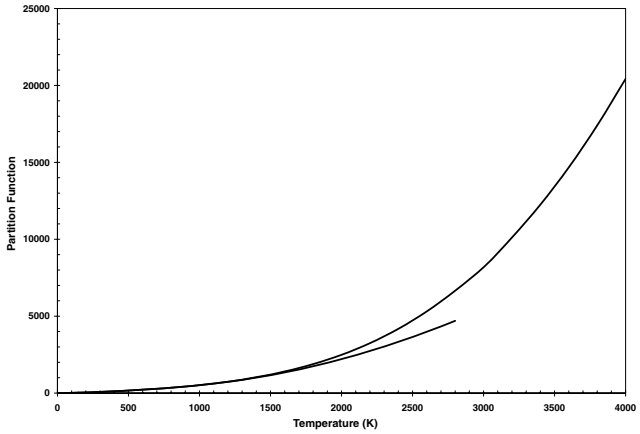

Figure 1. The H_2D^+ partition functions of ST1 (upper curve) and Sidhu et al. (1992) (lower curve).

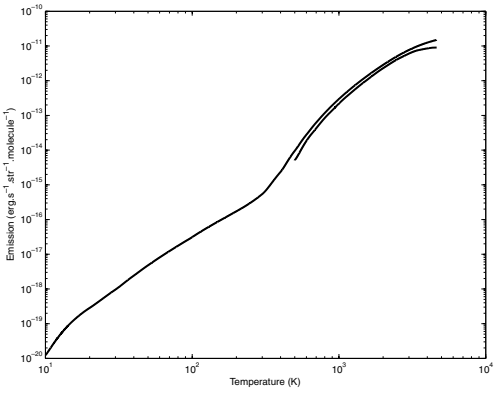

Figure 2. A graph of per molecule emission of H_2D^+ (upper curve) and H_3^+ (lower curve) as a function of temperature on a log–log scale. The H_2D^+ curve is obtained from ST1 while the H_3^+ curve is obtained from a digitized image from Neale et al. (1996).

where u and l stand for the upper and lower levels, respectively, and z is the partition function as given by equation (3). Fig. 2 graphically presents our cooling function as a function of temperature alongside the H_3^+ cooling function of Neale et al. (1996). As seen, the two curves are close for $T > 600$K. However, the H_2D^+ cooling function continues to be significant at lower temperatures, whereas at these temperatures the cooling curve of H_3^+ was not given by Neale et al. (1996) because they considered it too small to be of significance. This is of course why the cooling properties of H_2D^+ could be important in the early Universe. It should be remarked that

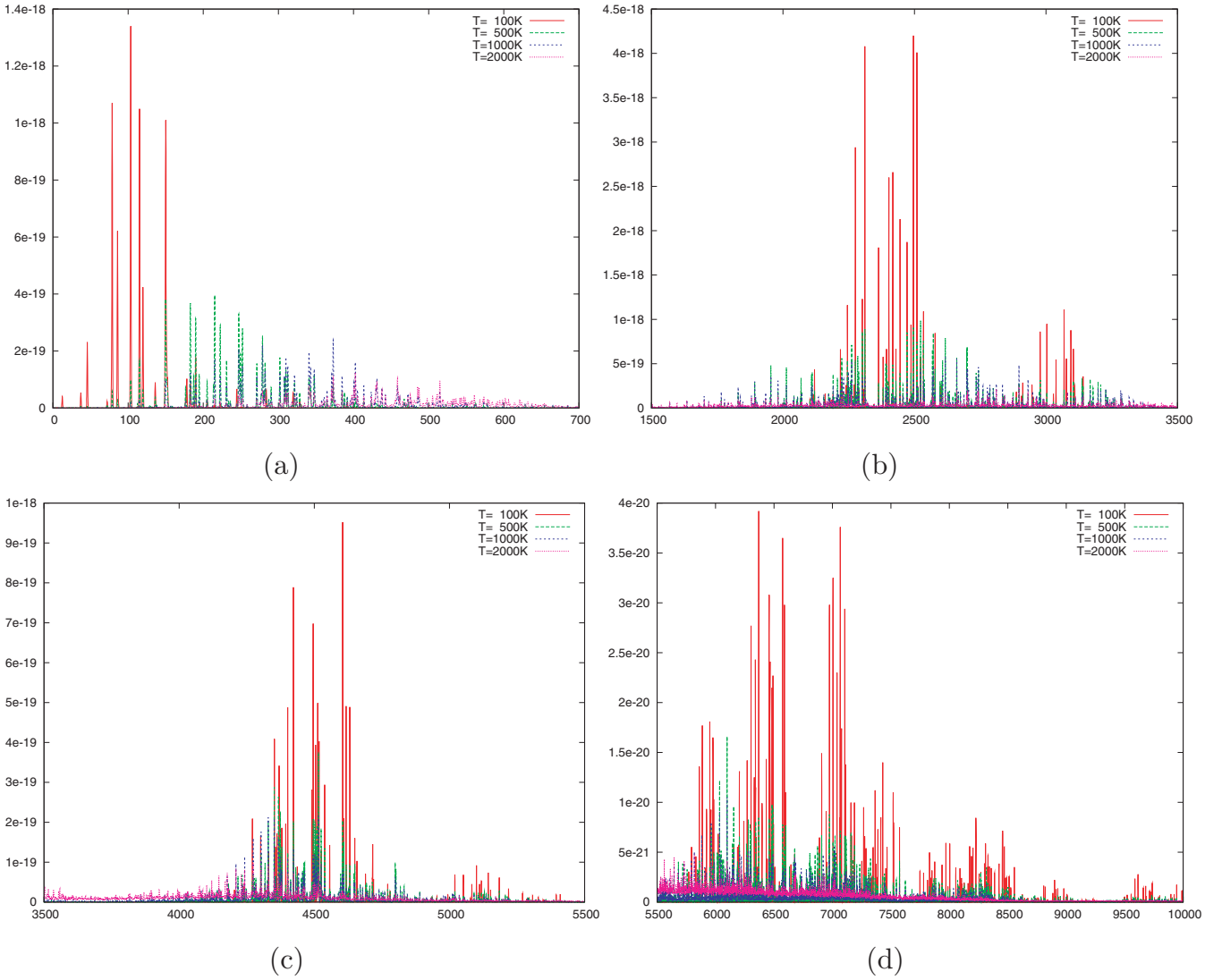

Figure 3. A graph of integrated absorption coefficient in cm molecule^{-1} (on y-axis) as a function of wavenumber in cm^{-1} (on x-axis) within the range 0–10 000 cm^{-1} for $T = 100$, 500, 1000 and 2000 K.

because of the low D/H ratio of about 10^{-5}, H_2D^+ will only become dominant at low temperatures below about 20 K where deuteration greatly enhances the H_2D^+ abundance.

Using a Levenberg–Marquardt curve-fitting routine, we fitted our H_2D^+ cooling function curve to a fourth-order polynomial in temperature over the range 10–4000 K and obtained

$$W(T) = \sum_{i=0}^{4} b_i T^i, \tag{7}$$

where

$$\begin{aligned} b_0 &= -1.343\,02 \times 10^{-16}, \\ b_1 &= +1.563\,14 \times 10^{-17}, \\ b_2 &= -2.697\,64 \times 10^{-19}, \\ b_3 &= +7.036\,02 \times 10^{-22}, \\ b_4 &= -1.108\,21 \times 10^{-25}. \end{aligned} \tag{8}$$

The fit was essentially perfect on a linear scale.

3.4 Synthetic Spectra

One of the main uses of line lists such as ST1 is to generate temperature-dependent synthetic spectra. We generated spectra from ST1 using the SPECTRA-BT2 code, which is described by Barber et al. (2006) and is a modified version of the original spectra code of Tennyson, Miller & Le Sueur (1993). Fig. 3(a) shows a temperature-dependent H_2D^+ absorption spectrum for the region largely associated with pure rotational transitions, while Figs 3(b)–(d) show the corresponding spectrum for the vibrational region. As is usual with rotation-vibration spectra, H_2D^+ spectra show a strong dependence on temperature.

4 CONCLUSIONS

In this paper we present a new line list (ST1) for the triatomic ion H_2D^+. The list, which can be obtained from the Centre de Données astronomiques de Strasbourg (CDS) data base at ftp://cdsarc.u-strasbg.fr/pub/cats/VI/130, comprises over 33 000 rotational-vibrational energy levels and more than 22 million transition lines archived within two files. The tests performed on the line

list suggest that, although it is based entirely on *ab initio* quantum mechanics, it should be accurate enough for almost all astronomical purposes. The one possible exception is for predicting the frequency of pure rotational transitions which are often needed to high accuracy and which are therefore better obtained from measured frequencies using combination differences.

5 ACKNOWLEDGEMENTS

We thank Lorenzo Lodi for his help with the DVR3D code and Steven Miller for encouraging to calculate H_2D^+ line list and for helpful discussions.

REFERENCES

Amano T., 1985, J. Opt. Soc. America B, 2, 790
Amano T., Hirao T., 2005, J. Molecular Spectrosc., 233, 7
Amano T., Watson J. K. G., 1984, J. Chemical Phys., 81, 2869
Asvany O., Hugo E., Müller F., Kühnemann F., Schiller S., Tennyson J., Schlemmer S., 2007, J. Chemical Phys., 127, 154317-1
Barber R. J., Tennyson J., Harris G. J., Tolchenov R. N., 2006, MNRAS, 368, 1087
Bogey M., Demuynck C., Denis M., Destombes J. L., Lemoine B., 1984, A&A, 137, L15
Boreiko R. T., Betz A. L., 1993, ApJ, 405, L39
Caselli P., van der Tak F. F. S., Ceccarelli C., Bacmann A., 2003, A&A, 403, L37
Caselli P., Vastel C., Ceccarelli C., van der Tak F. F. S., Crapsi A., Bacmann A., 2008, A&A, 492, 703
Ceccarelli C., Dominik C., 2006, ApJ, 640, L131
Ceccarelli C., Dominik C., Lefloch B., Caselli P., Caux E., 2004, ApJ, 607, L51
Cencek W., Rychlewski J., Jaquet R., Kutzelnigg W., 1998, J. Chemical Phys., 108, 2831
Cernicharo J., Polehampton E., Goicoechea J. R., 2007, ApJ, 657, L21
Dalgarno A., Herbst E., Novick S., Klemperer W., 1973, ApJ, 183, L131
Dubrovich V. K., 1993, Astron. Lett., 19, 53
Dubrovich V. K., Lipovka A. A., 1995, A&A, 296, 301
Dubrovich V., Partridge B., 2000, Astron. Astrophys. Trans., 19, 233
Fárník M., Davis S., Kostin M. A., Polyansky O. L., Tennyson J., Nesbitt D. J., 2002, J. Chemical Phys., 116, 6146
Foster S. C., McKellar A. R. W., Peterkin I. R., Watson J. K. G., Pan F. S., Crofton M. W., Altman R. S., Oka T., 1986, J. Chemical Phys., 84, 91
Galli D., Palla F., 1998, A&A, 335, 403
Harju J. et al., 2006, A&A, 454, L55
Herbst E., Millar T. J., 2008, in Smith I. W. M., ed., Low Temperatures and Cold Molecules. World Scientific, Singapore
Hlavenka P., Korolov I., Plašil R., Varju J., Kotrík T., Glosík J., 2006, Czechoslovak J. Phys., 56, B749
Hogerheijde M. R. et al., 2006, A&A, 454, L59
Millar T. J., 2003, Space Sci. Rev., 106, 73
Miller S., Tennyson J., Sutcliffe B. T., 1989, Molecular Phys., 66, 429
Neale L., Miller S., Tennyson J., 1996, ApJ, 464, 516
Pagani L. et al., 1992, A&A, 258, 472
Phillips T. G., Blake G. A., Keene J., Woods R. C., Churchwell E., 1985, ApJ, 294, L45
Polyansky O. L., Tennyson J., 1999, J. Chemical Phys., 110, 5056
Polyansky O. L., Prosmiti R., Klopper W., Tennyson J., 2000, Molecular Phys., 98, 261
Polyansky O. L., Császár A. G., Shirin S. V., Zobov N. F., Barletta P., Tennyson J., Schwenke D. W., Knowles P. J., 2003, Sci, 299, 539
Ramos A. A., Ceccarelli C., Elitzur M., 2007, A&A, 471, 187
Röhse R., Kutzelnigg W., Jaquet R., Klopper W., 1994, J. Chemical Phys., 101, 2231
Schinke R., Dupuis M., Lester W. A.Jr, 1980, J. Chemical Phys., 72, 3909
Schleicher D. R. G., Galli D., Palla F., Camenzind M., Klessen R. S., Bartelmann M., Glover S. C. O., 2008, A&A, 490, 521
Shy J.-T., Farley J. W., Wing W. H., 1981, Phys. Rev. A, 24, 1146
Sidhu K. S., Miller S., Tennyson J., 1992, A&A, 255, 453
Stark R., van der Tak F. F. S., van Dishoeck E. F., 1999, ApJ, 521, L67
Stark R. et al., 2004, ApJ, 608, 341
Tennyson J., Sutcliffe B. T., 1982, J. Chemical Phys., 77, 4061
Tennyson J., Sutcliffe B. T., 1983, J. Molecular Spectrosc., 101, 71
Tennyson J., Miller S., Le Sueur C. R., 1993, Comput. Phys. Communications, 75, 339
Tennyson J., Kostin M. A., Barletta P., Harris G. J., Polyansky O. L., Ramanlal J., Zobov N. F., 2004, Comput. Phys. Communications, 163, 85
van der Tak F. F. S., Caselli P., Ceccarelli C., 2005, A&A, 439, 195
van Dishoeck E. F., Phillips T. G., Keene J., Blake G. A., 1992, A&A, 261, L13
Vastel C., Phillips T. G., Yoshida H., 2004, ApJ, 606, L127
Warner H. E., Conner W. T., Petrmichl R. H., Woods R. C., 1984, J. Chemical Phys., 81, 2514
Yonezu T., Matsushima F., Moriwaki Y., Takagi K., Amano T., 2009, J. Molecular Spectrosc., 256, 238

This paper has been typeset from a TEX/LATEX file prepared by the author.